ATTITUDE DYNAMICS OF ON-ORBIT REFUELING CONFIGURATIONS*

Jing Pei† and Carlos M. Roithmayr‡

On-orbit refueling is a key enabling technology that will allow a significant increase in the amount of payload mass delivered beyond low-Earth orbit. Despite the potential benefits, there are numerous concerns regarding the operability and scalability of this critical technology. This paper explores the attitude dynamics of two docked spacecraft performing propellant transfer. A vector-dyadic equation is derived to account for the change over time in the mass distribution and the position of the mass center of the stack and moving mass terms omitted in previous literature. Subsequently, the result is applied to two SpaceX-inspired refueling configurations to assess the relative magnitudes of the various terms in the vector-dyadic equation in comparison to the gravity gradient torque.

INTRODUCTION

On-orbit refueling is a key enabling technology for delivering a significant amount of payload beyond low-Earth orbit (LEO) for exploration of the solar system. The mass of an exploration vehicle that can be delivered beyond LEO by a single heavy-lift launch vehicle is profoundly limited, as one can see by examining the rocket equation (Ref. [1]). On-orbit refueling circumvents this barrier by making it possible for the exploration vehicle to be launched at a fraction of the total wet mass. Subsequently, propellant is launched on multiple refueling flights and transferred to the exploration vehicle in LEO. While the performance benefits of on-orbit refueling are significant, a substantial increase in mission complexity cannot be overlooked. There are many concerns regarding operational reliability and logistics such as launch delays, failures, maintenance, propellant boil-off, rendezvous proximity operations and docking challenges (Ref. [2]). In order to mitigate the aforementioned risks, the NASA Tipping Point Program has awarded contracts to four industry partners for maturation of in-space propellant transfer technology as discussed in Refs. [3] and [4]. Figure 1 is an illustration of the SpaceX Starship Tail-to-Tail refueling configuration concept (Ref. [5]).

References [6] and [7] explore a list of enabling technologies necessary for on-orbit cryogenic propellant transfer. Propellant transfer can result in rapid changes in the stack mass distribution and center of mass position. For performing analysis of attitude dynamics and control it is important to assess the magnitude of the disturbance caused by propellant transfer and compare it to the typical on-orbit environmental disturbance torques, namely, gravity-gradient, aerodynamic drag, and solar

†Aerospace Engineer, Atmospheric Flight Entry Systems Branch, NASA Langley Research Center, Hampton, Virginia, 23681, USA.

‡Senior Aerospace Engineer, Vehicle Analysis Branch, NASA Langley Research Center, Hampton, Virginia, 23681, USA.

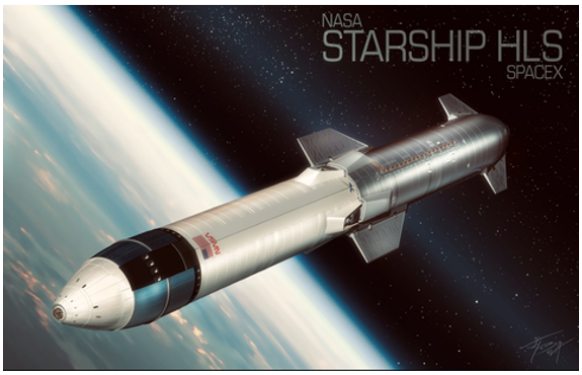

Figure 1. SpaceX Starship Tail-Tail Refueling Concept [5].

radiation pressure. To the best of the authors' knowledge, Refs. [8] and [9] are the only papers in the open literature that attempt to describe the detailed vehicle attitude dynamics during propellant transfer. Their approach is to modify Euler's rotational equations of motion for a rigid body by permitting the moments and products of inertia to vary with time. A rigorous application of the angular momentum principle, however, shows that this approach is flawed. As will be seen in what follows, terms have been incorrectly omitted from the system angular momentum and its time derivative in Refs. [8] and [9]. The purpose of this paper is to provide a corrected set of attitude dynamics equations so that control system engineers have better insight into the evolution of vehicle dynamics throughout the propellant transfer process and to enable design of a controller that will meet system requirements such as pointing error and minimization of propellant usage.

The remainder of the paper consists of three sections. In the first of these, the angular momentum principle is employed to obtain a vector-dyadic equation for the attitude dynamics of the dry portion of the vehicle stack. In the second section the vector-dyadic equation is implemented in matrix form and applied to the tail-tail and spine-spine on-orbit refueling concepts proposed by SpaceX (Ref. [10]) as part of the Human Landing System (HLS) mission architecture. This marks the first time propellant transfer between spacecraft of this size will be attempted. It is imperative that analyses account for all of the relevant physics in the attitude motion. Notional parameters are used to assess the magnitude of all terms in the attitude dynamics in comparison to gravity gradient torque for both refueling configurations. Conclusions are presented in the final section.

DYNAMICS

The dynamic system of interest is modeled as a single rigid body, B, together with an even number n of bodies $C_1, \ldots, C_n$, each of whose mass can vary with time but is otherwise regarded as rigid; each such body has a single translational degree of freedom relative to B. The two vehicles fixed to each other, with empty propellant tanks, are represented by B; their combined dry mass is denoted by m_B. As assumed in Ref. [8], C_i is a cylindrical tank containing propellant having mass m_i that can vary with time. Boil-off and leakage are neglected, so that the total propellant mass in the system does not change as it is transferred between tanks. Sloshing is ignored; the liquid is assumed to occupy a cylindrical volume whose height changes as the propellant is transferred.

The angular momentum in an inertial reference frame, N, of the system S with respect to the system mass center $S^\star$ is denoted by ${}^N\mathbf{H}^{S/S^\star}$ and can be referred to simply as the central angular

momentum of S in N. The angular momentum principle, expressed as

$$\frac{{}^N d\, {}^N\mathbf{H}^{S/S^\star}}{dt} = \mathbf{M} \tag{1}$$

states that the time derivative in N, denoted by ${}^N d/dt$, of ${}^N\mathbf{H}^{S/S^\star}$ is equal to the resultant moment $\mathbf{M}$ about $S^\star$ of the external forces applied to S.

The central angular momentum of S in N can be expressed as

$${}^N\mathbf{H}^{S/S^\star} = \underline{\mathbf{I}}^{B/B^\star} \cdot {}^N\boldsymbol{\omega}^B + m_B\, \mathbf{r}^{S^\star B^\star} \times {}^N\mathbf{v}^{B^\star} + \sum_{i=1}^{n} \left(\underline{\mathbf{I}}^{C_i/C_i^\star} \cdot {}^N\boldsymbol{\omega}^{C_i} + m_i\, \mathbf{r}^{S^\star C_i^\star} \times {}^N\mathbf{v}^{C_i^\star} \right) \tag{2}$$

where ${}^N\boldsymbol{\omega}^B$ is the angular velocity of B in N, $\mathbf{r}^{S^\star B^\star}$ is the position vector from $S^\star$ to $B^\star$, the mass center of B, ${}^N\mathbf{v}^{B^\star}$ is the velocity of $B^\star$ in N, and $\underline{\mathbf{I}}^{B/B^\star}$ is the inertia dyadic of B relative to $B^\star$, or simply the central inertia dyadic of B. The terms in the sum are defined similarly. The velocity ${}^N\mathbf{v}^{C_i^\star}$ of $C_i^\star$ in N can be expressed as

$${}^N\mathbf{v}^{C_i^\star} = {}^N\mathbf{v}^{B^\star} + {}^N\boldsymbol{\omega}^B \times \mathbf{r}^{B^\star C_i^\star} + {}^B\mathbf{v}^{C_i^\star} \qquad (i = 1, \ldots, n) \tag{3}$$

where $\mathbf{r}^{B^\star C_i^\star}$ is the position vector from $B^\star$ to $C_i^\star$, and the velocity ${}^B\mathbf{v}^{C_i^\star}$ of $C_i^\star$ in B is the time derivative in B of the position vector from a point fixed in B to $C_i^\star$ $(i = 1, \ldots, n)$. The terms in Eq. (2) that involve velocities can be written as

$$\begin{aligned} & m_B\, \mathbf{r}^{S^\star B^\star} \times {}^N\mathbf{v}^{B^\star} + \sum_{i=1}^{n} m_i\, \mathbf{r}^{S^\star C_i^\star} \times {}^N\mathbf{v}^{C_i^\star} \\ &= \left(m_B\, \mathbf{r}^{S^\star B^\star} + \sum_{i=1}^{n} m_i\, \mathbf{r}^{S^\star C_i^\star} \right) \times {}^N\mathbf{v}^{B^\star} + \sum_{i=1}^{n} m_i\, \mathbf{r}^{S^\star C_i^\star} \times \left({}^N\boldsymbol{\omega}^B \times \mathbf{r}^{B^\star C_i^\star} + {}^B\mathbf{v}^{C_i^\star} \right) \\ &= \sum_{i=1}^{n} m_i\, \mathbf{r}^{S^\star C_i^\star} \times \left({}^N\boldsymbol{\omega}^B \times \mathbf{r}^{B^\star C_i^\star} + {}^B\mathbf{v}^{C_i^\star} \right) \end{aligned} \tag{4}$$

The term in parentheses that precedes ${}^N\mathbf{v}^{B^\star}$ vanishes by virtue of the definition of the system mass center. The term in Eq. (4) that involves ${}^N\boldsymbol{\omega}^B$ can be expressed as

$$\sum_{i=1}^{n} m_i\, \mathbf{r}^{S^\star C_i^\star} \times \left({}^N\boldsymbol{\omega}^B \times \mathbf{r}^{B^\star C_i^\star} \right) = \sum_{i=1}^{n} m_i\, \mathbf{r}^{S^\star C_i^\star} \times \left[{}^N\boldsymbol{\omega}^B \times \left(\mathbf{r}^{B^\star S^\star} + \mathbf{r}^{S^\star C_i^\star} \right) \right] \tag{5}$$

Now, in view of Eqs. (3.5.31) and (3.6.9) of Ref. [11],

$$\begin{aligned} m_i\, \mathbf{r}^{S^\star C_i^\star} \times \left({}^N\boldsymbol{\omega}^B \times \mathbf{r}^{S^\star C_i^\star} \right) &= m_i \left[\underline{\mathbf{U}} \left(\mathbf{r}^{S^\star C_i^\star} \cdot \mathbf{r}^{S^\star C_i^\star} \right) - \mathbf{r}^{S^\star C_i^\star} \mathbf{r}^{S^\star C_i^\star} \right] \cdot {}^N\boldsymbol{\omega}^B \\ &\triangleq \underline{\mathbf{I}}^{C_i^\star/S^\star} \cdot {}^N\boldsymbol{\omega}^B \qquad (i = 1, \ldots, n) \end{aligned} \tag{6}$$

where $\underline{\mathbf{U}}$ is the unit dyadic. $\underline{\mathbf{I}}^{C_i^\star/S^\star}$ is the inertia dyadic relative to $S^\star$ of a (fictitious) particle of mass m_i placed at $C_i^\star$ (Ref. [11], p. 70); in other words, $\underline{\mathbf{I}}^{C_i^\star/S^\star}$ is a parallel axis term that, when added to $\underline{\mathbf{I}}^{C_i/C_i^\star}$, yields the inertia dyadic $\underline{\mathbf{I}}^{C_i/S^\star}$ of C_i relative to $S^\star$.

$$\underline{\mathbf{I}}^{C_i/S^\star} = \underline{\mathbf{I}}^{C_i/C_i^\star} + \underline{\mathbf{I}}^{C_i^\star/S^\star} \qquad (i = 1, \ldots, n) \tag{7}$$

The term on the right-hand side of Eq. (5) that has not yet been dealt with can be developed by appealing once more to the definition of the system mass center.

$$\begin{aligned}\sum_{i=1}^{n} m_i \, \mathbf{r}^{S^\star C_i^\star} \times \left({}^N\boldsymbol{\omega}^B \times \mathbf{r}^{B^\star S^\star} \right) &= -m_B \mathbf{r}^{S^\star B^\star} \times \left({}^N\boldsymbol{\omega}^B \times \mathbf{r}^{B^\star S^\star} \right) \\ &= m_B \mathbf{r}^{S^\star B^\star} \times \left({}^N\boldsymbol{\omega}^B \times \mathbf{r}^{S^\star B^\star} \right) \\ &= m_B \left[\underline{\mathbf{U}} \left(\mathbf{r}^{S^\star B^\star} \cdot \mathbf{r}^{S^\star B^\star} \right) - \mathbf{r}^{S^\star B^\star} \mathbf{r}^{S^\star B^\star} \right] \cdot {}^N\boldsymbol{\omega}^B \\ &\triangleq \underline{\mathbf{I}}^{B^\star/S^\star} \cdot {}^N\boldsymbol{\omega}^B \end{aligned} \tag{8}$$

The inertia dyadic of S relative to $S^\star$ (the central inertia dyadic of S) can be expressed as

$$\underline{\mathbf{I}}^{S/S^\star} = \underline{\mathbf{I}}^{B/B^\star} + \underline{\mathbf{I}}^{B^\star/S^\star} + \sum_{i=1}^{n} \left(\underline{\mathbf{I}}^{C_i/C_i^\star} + \underline{\mathbf{I}}^{C_i^\star/S^\star} \right) \tag{9}$$

Because body C_i can only translate relative to B, ${}^N\boldsymbol{\omega}^{C_i} = {}^N\boldsymbol{\omega}^B$ $(i = 1, \ldots, n)$. In that case, substitution from Eqs. (4), (5), (6), (8), and (9) into Eq. (2) yields

$${}^N\mathbf{H}^{S/S^\star} = \underline{\mathbf{I}}^{S/S^\star} \cdot {}^N\boldsymbol{\omega}^B + \sum_{i=1}^{n} m_i \, \mathbf{r}^{S^\star C_i^\star} \times {}^B\mathbf{v}^{C_i^\star} \tag{10}$$

The sum on the right-hand side of Eq. (10) appears to have been omitted by the authors of Refs. [8] and [9]. Equation (1) of Ref. [8] is evidently reproduced by incorrectly neglecting the sum when substituting from Eq. (10) into Eq. (1):

$$\frac{{}^B d\underline{\mathbf{I}}^{S/S^\star}}{dt} \cdot {}^N\boldsymbol{\omega}^B + \underline{\mathbf{I}}^{S/S^\star} \cdot \frac{{}^B d\, {}^N\boldsymbol{\omega}^B}{dt} + {}^N\boldsymbol{\omega}^B \times \left(\underline{\mathbf{I}}^{S/S^\star} \cdot {}^N\boldsymbol{\omega}^B \right) = \mathbf{M} \tag{11}$$

where ${}^B d/dt$ indicates taking the time derivative in B. A correct vector-dyadic equation for attitude dynamics must include the time derivative in N of the sum in Eq. (10).

$$\begin{aligned} &\frac{{}^B d\underline{\mathbf{I}}^{S/S^\star}}{dt} \cdot {}^N\boldsymbol{\omega}^B + \underline{\mathbf{I}}^{S/S^\star} \cdot \frac{{}^B d\, {}^N\boldsymbol{\omega}^B}{dt} + {}^N\boldsymbol{\omega}^B \times \left(\underline{\mathbf{I}}^{S/S^\star} \cdot {}^N\boldsymbol{\omega}^B \right) \\ &+ \sum_{i=1}^{n} \left[\dot{m}_i \, \mathbf{r}^{S^\star C_i^\star} \times {}^B\mathbf{v}^{C_i^\star} + m_i \left(\frac{{}^B d\mathbf{r}^{S^\star C_i^\star}}{dt} + {}^N\boldsymbol{\omega}^B \times \mathbf{r}^{S^\star C_i^\star} \right) \times {}^B\mathbf{v}^{C_i^\star} \right. \\ &\left. + m_i \, \mathbf{r}^{S^\star C_i^\star} \times {}^B\mathbf{a}^{C_i^\star} + m_i \, \mathbf{r}^{S^\star C_i^\star} \times \left({}^N\boldsymbol{\omega}^B \times {}^B\mathbf{v}^{C_i^\star} \right) \right] = \mathbf{M} \end{aligned} \tag{12}$$

where the acceleration ${}^B\mathbf{a}^{C_i^\star}$ of $C_i^\star$ in B is the time derivative in B of ${}^B\mathbf{v}^{C_i^\star}$, and $\dot{m}_i$ is the mass flow rate of the i^{th} tank. The contributions of the moving propellant to the attitude dynamics are magnified if the fuel mass fraction and mass flow rates are both significant. It is worth noting that terms in the sum vanish when certain vectors are parallel to each other. The time derivative in B of $\underline{\mathbf{I}}^{S/S^\star}$ can be expressed as

$$\frac{{}^B d\underline{\mathbf{I}}^{S/S^\star}}{dt} = \underline{\mathbf{0}} + \frac{{}^B d\underline{\mathbf{I}}^{B^\star/S^\star}}{dt} + \sum_{i=1}^{n} \left(\frac{{}^B d\underline{\mathbf{I}}^{C_i/C_i^\star}}{dt} + \frac{{}^B d\underline{\mathbf{I}}^{C_i^\star/S^\star}}{dt} \right) \tag{13}$$

where $\underline{\mathbf{0}}$ is the zero dyadic.

APPLICATION

In this section, terms in Eq. (12) are further developed for the tail-tail and spine-spine refueling configurations (Ref. [10]). Subsequently, notional vehicle and propellant parameters are used to assess the magnitudes of the terms in Eq. (12) for each configuration in comparison to gravity gradient torque, assuming a 300 km circular refueling orbit with an inclination of 30 deg and refueling duration of 90 minutes. To minimize propellant boiloff, a Sun pointing attitude is assumed for the duration of the transfer process. For simplicity it is assumed that a single liquid oxygen (LoX) tank is placed in the aft end of each vehicle, and the two vehicles have identical mass properties when the tanks are empty; vehicle 1 starts out with the LoX tank fully filled, whereas vehicle 2 starts out with the LoX tank empty.

Tail-Tail Configuration

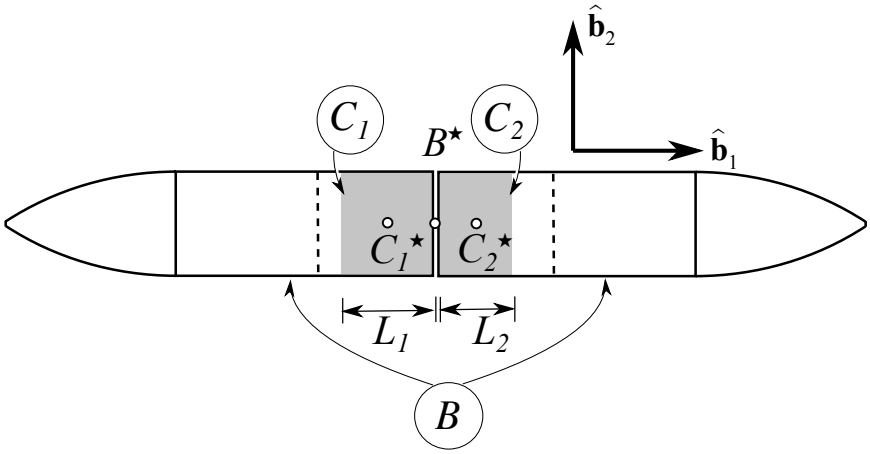

Figure 2. Tail-Tail Concept

A schematic of the tail-tail configuration is shown in Fig. 2. The dashed lines represent the 100% fill level of each tank and the shaded regions represent the volume of the liquid inside the tanks at a given time. Position vectors from $B^\star$ to $C_i^\star$, $B^\star$ to $S^\star$, and $S^\star$ to $C_i^\star$ are presented in Eqs. (14) through (16).

$$\begin{aligned} \mathbf{r}^{B^\star C_1^\star} &= -L_1/2\hat{\mathbf{b}}_1 = -\frac{m_1}{2S^2}\hat{\mathbf{b}}_1 \\ \mathbf{r}^{B^\star C_2^\star} &= L_2/2\hat{\mathbf{b}}_1 = \frac{m_2}{2S^2}\hat{\mathbf{b}}_1 \end{aligned} \tag{14}$$

$$\mathbf{r}^{B^\star S^\star} = \frac{-m_1 L_1 + m_2 L_2}{2m_T}\hat{\mathbf{b}}_1 = \frac{-m_1^2 + m_2^2}{2m_T S^2}\hat{\mathbf{b}}_1 \triangleq \lambda_t \hat{\mathbf{b}}_1 \tag{15}$$

$$\begin{aligned} \mathbf{r}^{S^\star C_1^\star} &= \left(-\frac{m_1}{2S^2} - \lambda_t\right)\hat{\mathbf{b}}_1 \\ \mathbf{r}^{S^\star C_2^\star} &= \left(\frac{m_2}{2S^2} - \lambda_t\right)\hat{\mathbf{b}}_1 \end{aligned} \tag{16}$$

where $S^2 = \rho\pi R^2$, ρ is the density of the liquid, R is the radius of the tank, and $m_T = m_B + \sum_{i=1}^{n} m_i$. Matrices associated with certain dyadics on the right-hand side of Eq. (9) are presented in Eqs. (17) – (19). For example, the matrix elements on the right-hand side of Eq. (17) are the dot products $\hat{\mathbf{b}}_r \cdot \underline{\mathbf{I}}^{B^\star/S^\star} \cdot \hat{\mathbf{b}}_s$ $(r, s = 1, 2, 3)$. In the interest of brevity, matrices associated with $\underline{\mathbf{I}}^{C_2/C_2^\star}$ and $\underline{\mathbf{I}}^{C_2^\star/S^\star}$ are not shown.

$$[\mathrm{I}]^{B^\star/S^\star} = m_B \begin{bmatrix} 0 & 0 & 0 \\ 0 & \lambda_t^2 & 0 \\ 0 & 0 & \lambda_t^2 \end{bmatrix} \tag{17}$$

$$[\mathrm{I}]^{C_1/C_1^\star} = m_1 \begin{bmatrix} \frac{1}{2}R^2 & 0 & 0 \\ 0 & \frac{1}{12}(3R^2 + m_1^2/S^4) & 0 \\ 0 & 0 & \frac{1}{12}(3R^2 + m_1^2/S^4) \end{bmatrix} \tag{18}$$

$$[\mathrm{I}]^{C_1^\star/S^\star} = m_1 \begin{bmatrix} 0 & 0 & 0 \\ 0 & \left[m_1/(2S^2) + \lambda_t\right]^2 & 0 \\ 0 & 0 & \left[m_1/(2S^2) + \lambda_t\right]^2 \end{bmatrix} \tag{19}$$

Equations (20) – (22) contain time derivatives of the matrix elements given in Eqs. (17) – (19), respectively.

$$\left[\dot{\mathrm{I}}\right]^{B^\star/S^\star} = 2m_B \begin{bmatrix} 0 & 0 & 0 \\ 0 & \lambda_t\dot{\lambda}_t & 0 \\ 0 & 0 & \lambda_t\dot{\lambda}_t \end{bmatrix} \tag{20}$$

$$\left[\dot{\mathrm{I}}\right]^{C_1/C_1^\star} = \begin{bmatrix} -\frac{1}{2}\dot{m}R^2 & 0 & 0 \\ 0 & -\frac{1}{4}\dot{m}(R^2 + m_1^2/S^4) & 0 \\ 0 & 0 & -\frac{1}{4}\dot{m}(R^2 + m_1^2/S^4) \end{bmatrix} \tag{21}$$

$$\left[\dot{\mathrm{I}}\right]^{C_1^\star/S^\star} = \begin{bmatrix} 0 & 0 & 0 \\ 0 & \eta & 0 \\ 0 & 0 & \eta \end{bmatrix} \tag{22}$$

where $\dot{\lambda}_t$ and η are given in Eqs. (23) and (24):

$$\dot{\lambda}_t = \frac{\dot{m}(-m_1 + m_2)}{m_T S^2} \tag{23}$$

$$\eta = 2m_1 \left(\frac{m_1}{2S^2} + \lambda_t\right)\left(-\frac{\dot{m}}{2S^2} + \dot{\lambda}_t\right) - \dot{m}\left(\frac{m_1}{2S^2} + \lambda_t\right)^2 \tag{24}$$

Spine-Spine Configuration

A schematic of the spine-spine configuration is shown in Fig. 3. Position vectors from $B^\star$ to $C_i^\star$, $B^\star$ to $S^\star$, and $S^\star$ to $C_i^\star$ are presented in Eqs. (25) through (27).

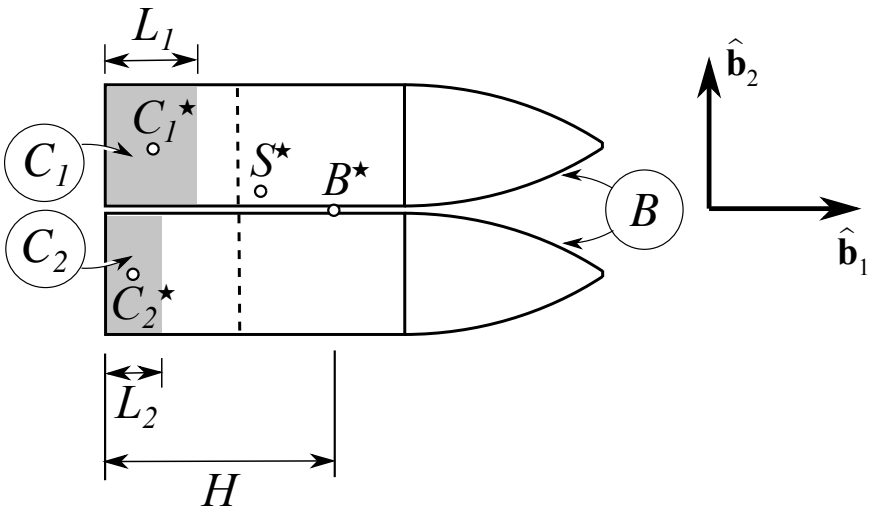

Figure 3. Spine-Spine Concept

$$\begin{aligned}\mathbf{r}^{B^\star C_1^\star} &= \left(-H + \frac{m_1}{2S^2}\right)\hat{\mathbf{b}}_1 + R\hat{\mathbf{b}}_2 \\ \mathbf{r}^{B^\star C_2^\star} &= \left(-H + \frac{m_2}{2S^2}\right)\hat{\mathbf{b}}_1 - R\hat{\mathbf{b}}_2\end{aligned} \tag{25}$$

$$\mathbf{r}^{B^\star S^\star} = \left[-\frac{H(m_1+m_2)}{m_T} + \frac{m_1^2+m_2^2}{2m_T S^2}\right]\hat{\mathbf{b}}_1 + \left[\frac{R(m_1-m_2)}{m_T}\right]\hat{\mathbf{b}}_2 \triangleq \lambda_s\hat{\mathbf{b}}_1 + \left[\frac{R(m_1-m_2)}{m_T}\right]\hat{\mathbf{b}}_2 \tag{26}$$

$$\begin{aligned}\mathbf{r}^{S^\star C_1^\star} &= \left(-\lambda_s - H + \frac{m_1}{2S^2}\right)\hat{\mathbf{b}}_1 + \left[R - \frac{R(m_1-m_2)}{m_T}\right]\hat{\mathbf{b}}_2 \\ \mathbf{r}^{S^\star C_2^\star} &= \left(-\lambda_s - H + \frac{m_2}{2S^2}\right)\hat{\mathbf{b}}_1 - \left[R + \frac{R(m_1-m_2)}{m_T}\right]\hat{\mathbf{b}}_2\end{aligned} \tag{27}$$

Matrices associated with certain dyadics on the right-hand side of Eq. (9) are presented in Eqs. (28) – (30), where $\gamma_1 = -\lambda_s - H + m_1/(2S^2)$. In the interest of brevity, matrices associated with $\underline{\mathbf{I}}^{C_2/C_2^\star}$ and $\underline{\mathbf{I}}^{C_2^\star/S^\star}$ are not shown.

$$[\mathrm{I}]^{B^\star/S^\star} = m_B\begin{bmatrix}\frac{R^2}{m_T^2}(m_1-m_2)^2 & \frac{-R}{m_T}(m_1-m_2)\lambda_s & 0 \\ \frac{-R}{m_T}(m_1-m_2)\lambda_s & \lambda_s^2 & 0 \\ 0 & 0 & \frac{R^2}{m_T^2}(m_1-m_2)^2 + \lambda_s^2\end{bmatrix} \tag{28}$$

$$[\mathrm{I}]^{C_1/C_1^\star} = m_1\begin{bmatrix}\frac{1}{2}R^2 & 0 & 0 \\ 0 & \frac{1}{12}(3R^2 + m_1^2/S^4) & 0 \\ 0 & 0 & \frac{1}{12}(3R^2 + m_1^2/S^4)\end{bmatrix} \tag{29}$$

$$[\mathrm{I}]^{C_1^\star/S^\star} = m_1 \begin{bmatrix} \frac{R^2}{m_T^2}(2m_2+m_B)^2 & -\frac{R}{m_T}(2m_2+m_B)\gamma_1 & 0 \\ -\frac{R}{m_T}(2m_2+m_B)\gamma_1 & \gamma_1^2 & 0 \\ 0 & 0 & \frac{R^2}{m_T^2}(2m_2+m_B)^2+\gamma_1^2 \end{bmatrix} \tag{30}$$

Time derivatives of the matrix elements given in Eqs. (28) – (30), respectively, are contained in Eqs. (31) – (33), where $\dot{\lambda}_s = \dot{m}(m_2-m_1)/\left(m_T S^2\right)$ and $\dot{\gamma}_1 = -\dot{\lambda}_s - \dot{m}/\left(2S^2\right)$.

$$\left[\dot{\mathrm{I}}\right]^{B^\star/S^\star} = \begin{bmatrix} \dot{\mathrm{I}}_{11}^{B^\star/S^\star} & \dot{\mathrm{I}}_{12}^{B^\star/S^\star} & 0 \\ \dot{\mathrm{I}}_{21}^{B^\star/S^\star} & 2m_B\lambda_s\dot{\lambda}_s & 0 \\ 0 & 0 & \dot{\mathrm{I}}_{33}^{B^\star/S^\star} \end{bmatrix} \tag{31}$$

where

$$\begin{aligned} \dot{\mathrm{I}}_{11}^{B^\star/S^\star} &= -4m_B\dot{m}\frac{R^2}{m_T^2}(m_1-m_2) \\ \dot{\mathrm{I}}_{12}^{B^\star/S^\star} &= -m_B\frac{R}{m_T}[(m_1-m_2)\dot{\lambda}_s - 2\dot{m}\lambda_s] \\ \dot{\mathrm{I}}_{21}^{B^\star/S^\star} &= \dot{\mathrm{I}}_{12}^{B^\star/S^\star} \\ \dot{\mathrm{I}}_{33}^{B^\star/S^\star} &= -4m_B\dot{m}\frac{R^2}{m_T^2}(m_1-m_2) + 2m_B\lambda_s\dot{\lambda}_s \end{aligned}$$

$$\left[\dot{\mathrm{I}}\right]^{C_1/C_1^\star} = \begin{bmatrix} -\frac{1}{2}\dot{m}R^2 & 0 & 0 \\ 0 & -\frac{1}{4}\dot{m}(R^2+m_1^2/S^4) & 0 \\ 0 & 0 & -\frac{1}{4}\dot{m}(R^2+m_1^2/S^4) \end{bmatrix} \tag{32}$$

$$\left[\dot{\mathrm{I}}\right]^{C_1^\star/S^\star} = \begin{bmatrix} \dot{\mathrm{I}}_{11}^{C_1^\star/S^\star} & \dot{\mathrm{I}}_{12}^{C_1^\star/S^\star} & 0 \\ \dot{\mathrm{I}}_{21}^{C_1^\star/S^\star} & \dot{\mathrm{I}}_{22}^{C_1^\star/S^\star} & 0 \\ 0 & 0 & \dot{\mathrm{I}}_{33}^{C_1^\star/S^\star} \end{bmatrix} \tag{33}$$

where

$$\begin{aligned} \dot{\mathrm{I}}_{11}^{C_1^\star/S^\star} &= \dot{m}\frac{R^2}{m_T^2}\Big[4m_1(2m_2+m_B) - (2m_2+m_B)^2\Big] \\ \dot{\mathrm{I}}_{12}^{C_1^\star/S^\star} &= m_1\Big\{-\frac{R}{m_T}\Big[\dot{\gamma}_1(2m_2+m_B) + 2\dot{m}\gamma_1\Big]\Big\} + \frac{R}{m_T}\Big[\dot{m}\gamma_1(2m_2+m_B)\Big] \\ \dot{\mathrm{I}}_{21}^{C_1^\star/S^\star} &= \dot{\mathrm{I}}_{12}^{C_1^\star/S^\star} \\ \dot{\mathrm{I}}_{22}^{C_1^\star/S^\star} &= 2m_1\gamma_1\dot{\gamma}_1 - \dot{m}\gamma_1^2 \\ \dot{\mathrm{I}}_{33}^{C_1^\star/S^\star} &= \dot{\mathrm{I}}_{11}^{C_1^\star/S^\star} + \dot{\mathrm{I}}_{22}^{C_1^\star/S^\star} \end{aligned}$$

Numerical Results

Parameters for the single vehicle are provided in Table 1 and Eq. (34). For a 90-minute refueling duration, $\dot{m}$ is approximately 185 kg/s. A fictitious future date was selected such that the desired Sun-pointing attitude can be determined. For completeness, a vector-dyadic expression for gravity gradient torque is provided in Eq. (35), where $\mathbf{R}_c$ is the position vector from the center of the Earth to $S^\star$, G is the universal gravitational constant, and m_e is the mass of the Earth. One may refer to Eq. (2.6.3) of Ref. [12] or Eq. (4.132) of Ref. [13].

Table 1. System Parameters

Parameter	Value
m_B	1.2×10^5 kg
R	4.5 m
H	14 m
ρ	1141 kg/m^3

$$[\mathrm{I}]^{B/B^\star} = \begin{bmatrix} 2.02 \times 10^6 & 1.2 \times 10^4 & -6.9 \times 10^4 \\ 1.2 \times 10^4 & 2.8 \times 10^7 & 1.03 \times 10^5 \\ -6.9 \times 10^4 & 1.03 \times 10^5 & 2.8 \times 10^7 \end{bmatrix} \text{kg-m}^2 \tag{34}$$

$$\mathbf{M}_G = \frac{3Gm_e}{\mathbf{R}_c^5} \mathbf{R}_c \times \underline{\mathbf{I}}^{S/S^\star} \cdot \mathbf{R}_c \tag{35}$$

Figure 4 shows the $\hat{\mathbf{b}}_1$ component of the relevant position vectors for the tail-tail configuration. A near 12 m shift in the axial position of the center of mass is predicted. For reference, the total length of a single vehicle is 45 m. Time histories of the central inertia matrix elements of S are shown in Fig. 5. Due to the axisymmetric nature of the configuration, only the 22 and 33 elements of $[\mathrm{I}]^{S/S^\star}$ vary with time. Note that the placement of the plots in Fig. 5 corresponds to the placement of the elements in the central inertia matrix.

Components of Eq. (12) in the $\hat{\mathbf{b}}_1$, $\hat{\mathbf{b}}_2$, and $\hat{\mathbf{b}}_3$ directions, respectively, are shown in Fig. 6 along with the expected gravity gradient torque. The first three terms represent the typical Euler's equation with time-varying inertia; T_1 through T_4 represent the four terms inside the sum in Eq. (12) due to moving propellant. For the tail-tail configuration, all the terms in the sum of Eq. (12) vanish because certain vectors involved in the cross products are parallel. Furthermore, the third term inside the brackets, $m_i \, \mathbf{r}^{S^\star C_i^\star} \times {}^B\mathbf{a}^{C_i^\star}$, is generally zero because a constant mass flow rate is desired. The terms in the typical Euler's equation also vanish because an inertial pointing attitude is prescribed, hence ${}^N\boldsymbol{\omega}^B = \mathbf{0}$ and ${}^B d\,{}^N\boldsymbol{\omega}^B/dt = \mathbf{0}$. Gravity gradient is the sole surviving component of Eq. (12). A slightly more interesting result is presented in Fig. 7 as the vehicle is prescribed to follow a constant 0.028 deg/s slew profile about $\hat{\mathbf{b}}_2$. $\hat{\mathbf{b}}_2$ components of Eq. (12) are shown (and magnified) to illustrate the second and fourth terms in the sum of Eq. (12) and $\dot{\mathrm{I}}\omega$ are non-zero. However, these are still small in comparison to the $\mathrm{I}\dot{\omega}$ and gravity gradient terms for the assumed conditions.

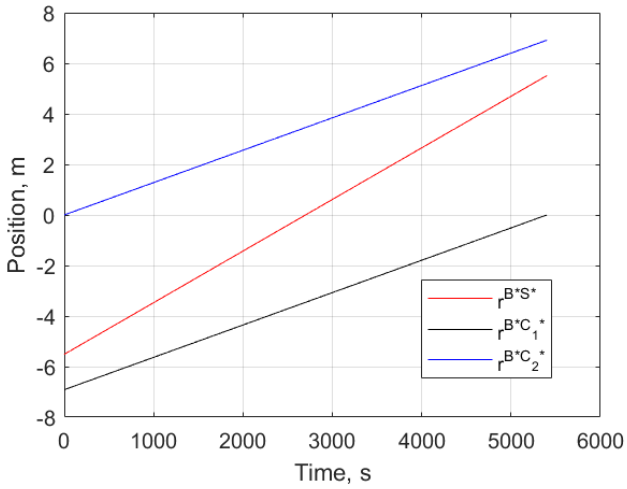

Figure 4. $\hat{\mathrm{b}}_1$ Component of the Position Vectors: Tail-Tail Configuration

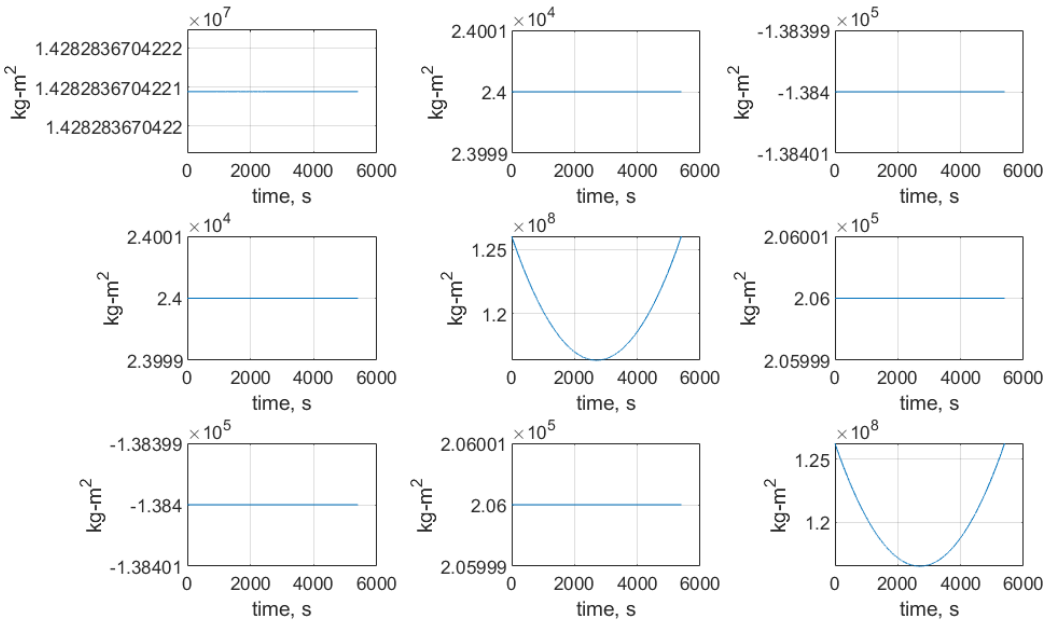

Figure 5. Central Inertia Matrix Elements of S, $[\mathrm{I}]^{S/S^\star}$: Tail-Tail Configuration

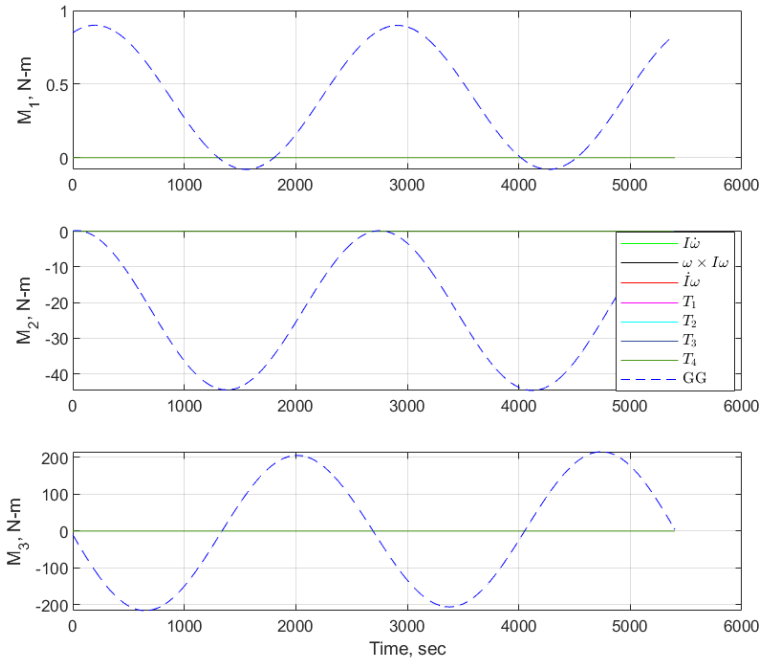

Figure 6. Components of Terms in Eq. (12), Sun-pointing: Tail-Tail Configuration

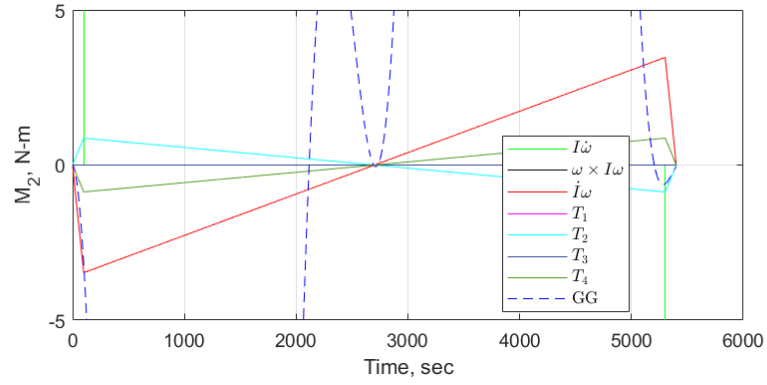

Figure 7. $\hat{b}_2$ Components of Eq. (12), slew maneuver about $\hat{b}_2$: Tail-Tail Configuration

Figure 8 shows the $\hat{\mathbf{b}}_1$ and $\hat{\mathbf{b}}_2$ components of the relevant position vectors for the spine-spine configuration. The absolute value of $\hat{\mathbf{b}}_1$ component of $\mathbf{r}^{B^\star/S^\star}$ is at its maximum at the midway point of the transfer while a shift in $S^\star$ of approximately 8 m parallel to $\hat{\mathbf{b}}_2$ is predicted. Time histories of the central matrix elements of S are shown in Fig. 9. Due to the lateral shift in the center of mass during the transfer, only the 23 and 32 elements of $[\mathrm{I}]^{S/S^\star}$ are non-zero. Components of Eq. (12) in the $\hat{\mathbf{b}}_1$, $\hat{\mathbf{b}}_2$, and $\hat{\mathbf{b}}_3$ directions, respectively, are shown in Fig. 10 along with the expected gravity gradient torque. Unlike the tail-tail configuration, the $\hat{\mathbf{b}}_3$ component of the first and second terms in the sum of Eq. (12) are non-zero, albeit small compared to gravity gradient.

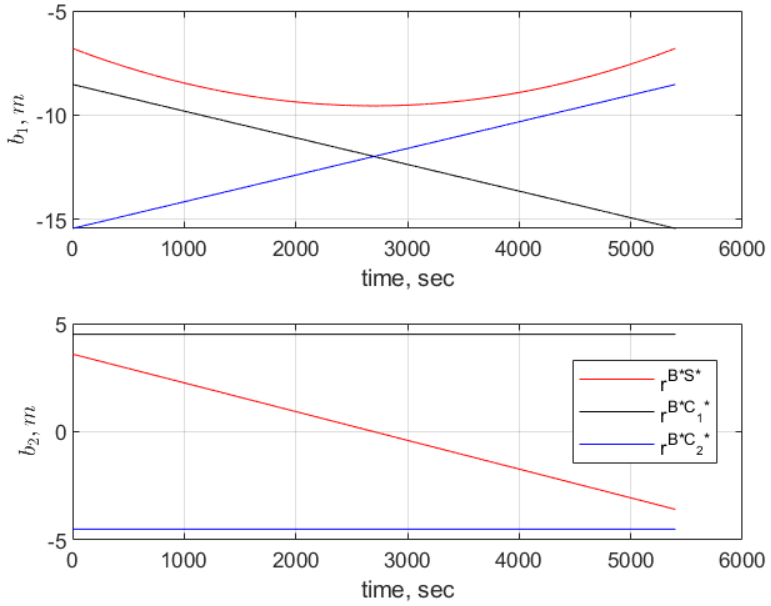

Figure 8. Components of the Position Vectors Parallel to $\hat{\mathbf{b}}_1$ and $\hat{\mathbf{b}}_2$: Spine-Spine Configuration

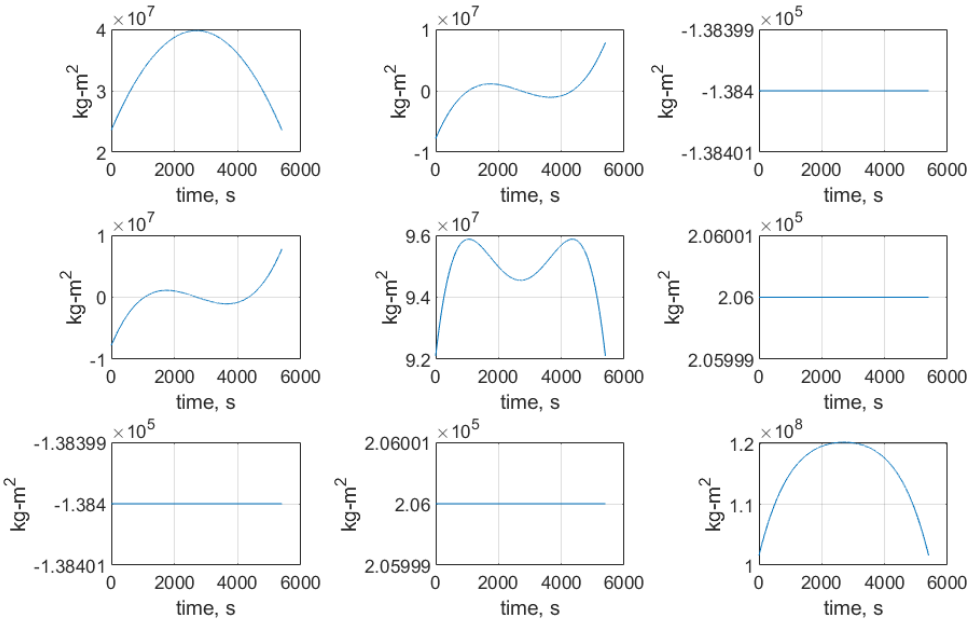

Figure 9. Central Inertia Matrix Elements of S, $[\mathrm{I}]^{S/S^\star}$: Spine-Spine Configuration

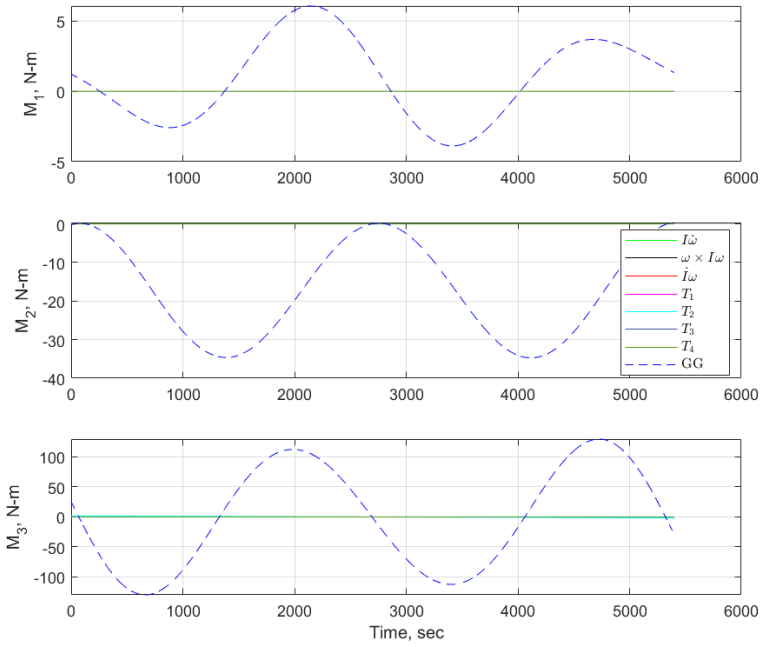

Figure 10. Components of Terms in Eq. (12), Sun-pointing: Spine-Spine Configuration

CONCLUSION

As demand for increasing payload capability beyond low-Earth orbit grows, mastery of on-orbit refueling becomes essential. A vector-dyadic equation is derived from first principles to study the attitude dynamics of two docked spacecraft performing propellant transfer. The complete equation accounts for the change over time in the stack's mass distribution, position of the center of mass, and terms associated with moving mass. In contrast to previous attempts, the current derivation includes the contributions of relative velocities and accelerations of the propellant masses to the time rate of change in angular momentum about the system mass center. The contributions of these effects to the attitude dynamics are magnified if the fuel mass fraction and mass flow rates are both significant. The result is applied to two SpaceX-inspired refueling configurations, tail-to-tail and spine-to-spine, to assess the relative magnitudes of the various terms in the vector-dyadic equation in comparison to the gravity gradient torque while assuming a Sun-pointing attitude. For the assumed vehicle and propellant transfer parameters the terms in the attitude equation are small in comparison to gravity gradient torque.

REFERENCES

[1] Thomson, W. T., *Introduction to Space Dynamics*, Dover Publications, Mineola, NY. 2000, pp. 242.

[2] Cirillo, W., Stromgren, C., and Gates, G., "Risk Analysis of On-Orbit Spacecraft Refueling Concepts," AIAA 2010-8832, AIAA Space Conference & Exposition, August 30 – September 2, 2010.

[3] https://www.nasa.gov/directorates/spacetech/solicitations/tipping_points/2020_selections [accessed 10 March, 2020].

[4] https://spaceflightnow.com/2020/10/16/nasa-selects-companies-to-demonstrate-in-space-refueling-and-propellant-depot-tech/ [accessed 10 March, 2020].

[5] https://www.reddit.com/r/elonmusk/comments/p30hjy/all_the_proposed_starship_orbital_refuel/ [accessed 30 May, 2022]

[6] Kutter, B., Zegler, F., et. al "Settled Cryogenic Propellant Transfer," AIAA 2006-4436, AIAA Joint Propulsion Conference & Exhibit, July 9–12, 2006.

[7] Chato, D., "Low Gravity Issues of Deep Space Refueling," AIAA 2005-1148, AIAA Aerospace Sciences Meeting and Exhibit, Jan 10–13, 2005.

[8] Guang, Z., Zheng, H., and Liang, B., "Attitude Dynamics of Spacecraft with Time-Varying Inertia During On-Orbit Refueling," *Journal of Guidance, Control, and Dynamics*, Vol. 41, No. 8, 2018, pp. 1744–1754.

[9] Xu, Y., "Adaptive attitude-tracking control of spacecraft considering on-orbit refueling," *Transations of the Institute of Measurement and Control*, Vol. 43, 2021, pp. 1298-1309.

[10] https://www.teslarati.com/spacex-how-to-refuel-starships-in-space/ [accessed 10 March, 2022]

[11] Kane, T. R., and Levinson, D. A., *Dynamics: Theory and Applications*, McGraw-Hill, New York, 1985, Chap. 3.

[12] Kane, T. R., Likins, P. W., and Levinson, D. A., *Spacecraft Dynamics*, McGraw-Hill, New York, 1983, p. 113.

[13] Schaub, H., and Junkins, L. J., *Analytical Mechanics of Space Systems*, AIAA, Reston, VA. 2003, pp. 160–162.